

Self-Aligned Supported Lipid Bilayers for Patterning the Cell–Substrate Interface

Keyue Shen, Jones Tsai, Peng Shi, and Lance C. Kam*

Department of Biomedical Engineering, Columbia University, New York, New York 10027

Received June 9, 2009; E-mail: lk2141@columbia.edu

Substrate supported lipid bilayers (SLBs) capture the fluidity of cellular membranes *in vitro*, providing a powerful tool for investigating protein mobility in cell signaling.^{1–9} This system has been applied most prominently to studies of T lymphocyte function;^{1,2} the SLB mimics an antigen presenting cell (APC) by presenting tethered proteins to receptors on the T cell. The receptor/ligand signaling clusters that form within the small (5–10 μm diameter) area of contact between T cell and SLB organize into complex patterns capturing the natural T cell/APC interface, a region termed the “immune synapse” (IS). As a specific example, these patterns include a concentric bull’s-eye configuration in which T Cell Receptor (TCR) and LFA-1 clusters localize to the center and periphery, respectively, of the IS.^{10–13} Surprisingly, this configuration emerges from a more transient structure, in which LFA-1 clusters are in the center of the IS, surrounded by TCR; notably, this rearrangement would not be possible in the absence of ligand mobility provided by the SLB. The factors that drive the inversion of this structure and other dynamics of the IS, as well as their impacts on cell function, are the topic of current research. Recent studies have shown that patterning the engagement of receptors on the T cell using surface-immobilized ligands modulates cell responses including migration and cytokine secretion.^{14–16} However, a system that provides similar control while retaining the lateral mobility that is essential for IS dynamics remains elusive; intermixing of ligands hinders the ability to precisely define biomolecular layout. Moreover, membrane topology and convergence of downstream signaling pathways complicate interpretation of cell function when ligands are locally mixed. The ability to present multiple, membrane-tethered ligands to T cells within the IS while minimizing the background presence of other ligands would greatly accelerate understanding of the IS.

Toward this goal, we introduce a simple approach for aligning multiple bilayer regions, each occupying a different lateral region of a single surface and presenting a different composition, by combining diffusive transport in SLBs with an appropriately designed barrier system to enhance the pattern resolution.¹⁷ The basic strategy is outlined in Figure 1A. A bilayer-compatible substrate (e.g., glass, mica, or silicon oxide) is divided into two open regions (zones 1 and 2) separated by a third (zone 3) containing a continuous barrier. The barrier divides the surface into two topologically distinct but interdigitating regions. Bilayers of different compositions are then formed on the three zones: two different target biomolecules (illustrated by the red and green tethered forms) are deposited on zones 1 and 2, while a plain bilayer is formed on zone 3. Over time, the red and green target molecules diffuse into the interdigitated region. This approach offers several advantages for creating multicomponent bilayer systems. Most importantly, spatial resolution is determined by the barrier in zone 3, reaching into scales of tens of nanometers.¹⁸ By comparison, microfluidic and microcontact printing approaches that have been used to directly pattern SLBs are limited to relatively low resolution

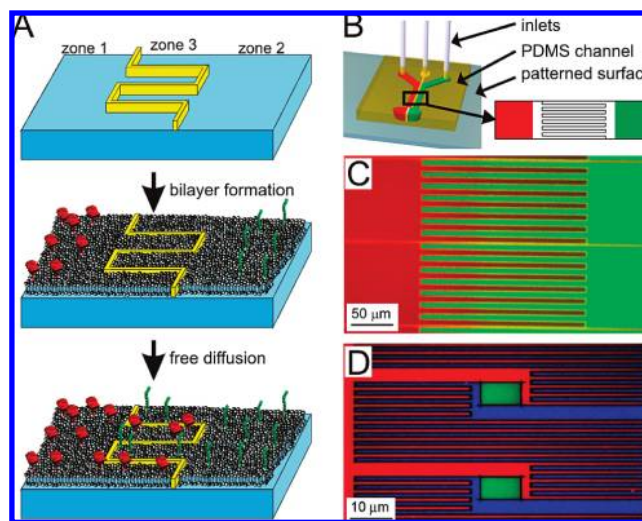


Figure 1. (A) Schematic illustrating self-aligning patterns of multiple SLBs. (B) A three-stream, converging laminar flow configuration used to define patterns of bilayer formation on micropatterned surfaces. (C) Interdigitation of bilayer regions, imaged 3 h after formation. The bilayers consisted of PC/TR (red) and PC/NBD (green) lipid mixtures and were separated by a barrier of AZ 5214 photoresist. (D) A finer three-component pattern with submicrometer resolution was achieved using e-beam lithography. The use of a more complicated barrier geometry allowed patterning of an increasing number of proteins. This surface was exposed to vesicles of PC/TR (red), PC/NBD (green), or PC-DiD (blue).

(3–10 μm);^{17,19–21} studies of T cell function in particular require the higher resolution provided by the method described here. Scanning probe techniques provide submicrometer resolution of SLBs^{22–24} but are not well-suited for covering the relatively large areas required for cell-based experiments. Second, there are few restrictions on the fabrication technique; any of the established barrier materials, including metals, photoresists, or proteins,^{25,26} can be used. Finally, this strategy requires a single bilayer deposition step, rather than one step for each different component.

This approach is demonstrated in Figure 1B–D. A three-channel, laminar-flow chamber of polydimethylsiloxane (Sylgard 184, Dow Corning) was used to deposit vesicles on a prepatterned surface (Figure 1B). For visualization, egg phosphatidylcholine (PC, Avanti Polar Lipids, Alabaster, AL) vesicles were supplemented with 0.5–2 mol % of Texas-Red labeled DHPE (TR, Molecular Probes, Portland, OR), NBD-PE (NBD, Avanti), or DiD (Molecular Probes). Figure 1C shows a relatively low-resolution demonstration of this process; a silicon wafer with a 250-nm oxide layer was patterned with a 1.5- μm wide serpentine barrier of an AZ 5214 photoresist, dividing the surface into two regions separated by a 200- μm -wide interdigitating region. Horizontal runs were spaced at 5- μm intervals. Figure 1C shows the surface 3 h after formation of the bilayer, illustrating interdigitation of the outer two lipid bilayers.

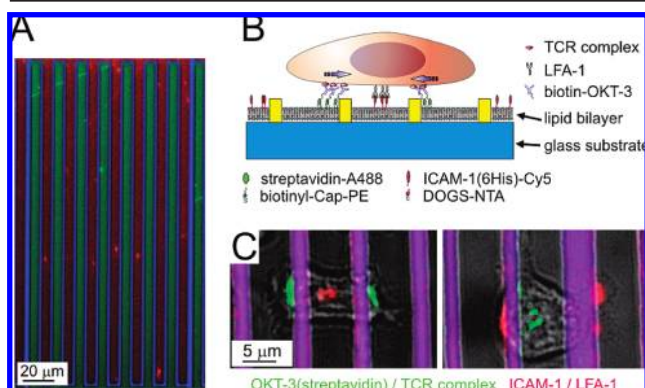


Figure 2. (A) Interdigitating bilayers used for capture of TCR and LFA-1 ligands. The barrier consists of S1805 photoresist (blue). DOPC SLBs were supplemented with biotinyl-Cap-PE or DOGS-NTA lipids. After overnight diffusion, streptavidin (green) and GFP-6His (red) were captured onto the bilayer surface. (B) Schematic illustration of T cell interaction with an interdigitated lipid bilayer presenting separated TCR activating and ICAM-1 adhesion signals. The arrows indicate the direction which T cells pull their ligands. (C) Human CD4⁺ T cell blasts interact with spatially separated ligands, forming altered IS configurations on the interdigitating bilayer. These representative images show 30-min interaction of T cells with the bilayers.

The photoresist barrier appears yellow in this image, as AZ 5214 is fluorescent in both TR and NBD channels (as confirmed by microscopy in the absence of fluorescently labeled lipids). Figure 1D illustrates a further evolution of this strategy to a higher resolution, three-component system (as detailed in Supporting Information). Electron-beam lithography was used to define a 100-nm-wide barrier of chromium (which appear dark) on glass that also incorporates rectangular regions topologically isolated from the rest of the pattern and subsequently located under the central stream of a laminar flow system. Bilayers formed inside these isolated regions (green) did not mix with other areas, while those in the central flow but outside the isolated rectangle were diluted into the adjacent bilayers, yielding the three-component system. Systems containing four or more membrane types can be readily envisioned (see Supporting Information).

We next demonstrate the use of our platform in presenting spatially segregated, micropatterned ligands to the T cell surface proteins TCR and LFA-1. A barrier (S1805 photoresist) was used to create a two-component, interdigitated system (Figure 2A) consisting of 1,2-dioleoyl-*sn*-glycero-3-phosphocholine (DOPC, Avanti) lipids supplemented with 0.02 mol % Biotinyl-Cap-PE (Avanti) on one side and 6 mol % of DOGS-NTA (Avanti) on the other. The S1805 photoresist exhibits fluorescence in the far-red spectrum, allowing better visualization of the resultant surface. The surface was blocked with BSA and incubated with Alexa-488 conjugated streptavidin (Molecular Probes), washed with PBS, and incubated with monobiotinylated-OKT3 (an antibody directed against and which activates TCR) and Cy5-labeled ICAM-1-6His (ICAM-1 is the natural ligand of LFA-1). The diffusion coefficient of ICAM-1 was determined to be $0.39 \mu\text{m}^2/\text{s}$ while that of streptavidin before and after linkage with biotin-OKT3 was 0.37 and $0.23 \mu\text{m}^2/\text{s}$, respectively.

Human CD4⁺ T cell blasts clustered the tethered ligands within minutes of introduction to the surface, spanning across up to three lipid bilayer stripes (Figure 2C); of 121 cells observed across two independent experiments, 51 interacted with a single stripe containing OKT3, 44 interacted with two bilayer stripes (one of OKT3 and a second of ICAM-1), while 26 spanned across three stripes

(Figure 2C). All cells formed clusters of OKT3 and ICAM-1, which were present only on the corresponding type of bilayer; cells were not able to pull ligands over the barriers over the 2 h observation time. Receptor clusters appeared to be directed toward the cell center, accumulating against barriers when this motion would be impeded or under the cell center in the absence of barriers. Cells overlying three stripes (Figure 2C) were able to form clusters of OKT3 or ICAM-1 in the central region, away from the bilayer edges. Notably, the ability of these cells to form ICAM-1 clusters which did not localize to the periphery of the IS suggests that the segregation observed in the normal IS is dependent on the concurrent presentation of TCR clusters in the same region; our system provides a new glimpse into this crosstalk, which will be investigated in subsequent studies. Cells were not able to attach to surfaces without tethered OKT3 and ICAM-1, showing that the barriers did not directly promote cell interaction.

In conclusion, the complex interplay between lateral mobility and spatial organization of signaling complexes is an emerging area of research. We introduce a new strategy for combining multiple, spatially separated SLBs on a single surface, with application specifically in the context of T cells.

Acknowledgment. We thank G. Vasiliver-Shamis, D. Blair, and M. L. Dustin (New York University School of Medicine) for CD4⁺ T cells and protein reagents. This work was supported by the National Institutes of Health, EY016586 and EB008199.

Supporting Information Available: Experimental procedures. This material is available free of charge via the Internet at <http://pubs.acs.org>.

References

- (1) Grakoui, A.; Bromley, S. K.; Sumen, C.; Davis, M. M.; Shaw, A. S.; Allen, P. M.; Dustin, M. L. *Science* **1999**, *285*, 221–7.
- (2) Groves, J. T.; Dustin, M. L. *J. Immunol. Methods* **2003**, *278*, 19–32.
- (3) Mossman, K. D.; Campi, G.; Groves, J. T.; Dustin, M. L. *Science* **2005**, *310*, 1191–3.
- (4) Pautot, S.; Lee, H.; Isacoff, E. Y.; Groves, J. T. *Nat. Chem. Biol.* **2005**, *1*, 283.
- (5) Perez, T. D.; Nelson, W. J.; Boxer, S. G.; Kam, L. *Langmuir* **2005**, *21*, 11963–68.
- (6) Oliver, A. E.; Ngassam, V.; Dang, P.; Sanii, B.; Wu, H.; Yee, C. K.; Yeh, Y.; Parikh, A. N. *Langmuir* **2009**, *25*, 6992–96.
- (7) Dori, Y.; Bianco-Peled, H.; Satija, S. K.; Fields, G. B.; McCarthy, J. B.; Tirrell, M. J. *Biomed. Mater. Res.* **2000**, *50*, 75–81.
- (8) Stroumpoulis, D.; Zhang, H.; Rubalcava, L.; Gliem, J.; Tirrell, M. *Langmuir* **2007**, *23*, 3849–56.
- (9) Yokosuka, T.; Kobayashi, W.; Sakata-Sogawa, K.; Takamatsu, M.; Hashimoto-Tane, A.; Dustin, M. L.; Tokunaga, M.; Saito, T. *Immunity* **2008**, *29*, 589–601.
- (10) Dustin, M. L. *Arthritis Res.* **2002**, *4*, S119–25.
- (11) Dustin, M. L.; Tseng, S. Y.; Varma, R.; Campi, G. *Curr. Opin. Immunol.* **2006**, *18*, 512–6.
- (12) Tseng, S. Y.; Liu, M.; Dustin, M. L. *J. Immunol.* **2005**, *175*, 7829–36.
- (13) Tseng, S. Y.; Waite, J. C.; Liu, M.; Vardhana, S.; Dustin, M. L. *J. Immunol.* **2008**, *181*, 4852–63.
- (14) Doh, J.; Irvine, D. J. *Proc. Natl. Acad. Sci. U.S.A.* **2006**, *103*, 5700–5.
- (15) Schwarzenbacher, M.; Kaltenbrunner, M.; Brameshuber, M.; Hesch, C.; Paster, W.; Weghuber, J.; Heise, B.; Sonnleitner, A.; Stockinger, H.; Schutz, G. J. *Nat. Methods* **2008**, *5*, 1053–60.
- (16) Shen, K.; Thomas, V. K.; Dustin, M. L.; Kam, L. C. *Proc. Natl. Acad. Sci. U.S.A.* **2008**, *105*, 7791–6.
- (17) Kam, L.; Boxer, S. G. *Langmuir* **2003**, *19*, 1624–1631.
- (18) Tsai, J.; Sun, E.; Gao, Y.; Hone, J. C.; Kam, L. C. *Nano. Lett.* **2008**, *8*, 425–30.
- (19) Kam, L.; Boxer, S. G. *J. Am. Chem. Soc.* **2000**, *122*, 12901–12902.
- (20) Yoshina-Ishii, C.; Boxer, S. G. *J. Am. Chem. Soc.* **2003**, *125*, 3696–7.
- (21) Yang, T.; Simanek, E. E.; Cremer, P. *Anal. Chem.* **2000**, *72*, 2587–9.
- (22) Jackson, B. L.; Groves, J. T. *J. Am. Chem. Soc.* **2004**, *126*, 13878–9.
- (23) Lenhert, S.; Sun, P.; Wang, Y.; Fuchs, H.; Mirkin, C. A. *Small* **2007**, *3*, 71–5.
- (24) Shi, J.; Chen, J.; Cremer, P. S. *J. Am. Chem. Soc.* **2008**, *130*, 2718–9.
- (25) Kung, L. A.; Kam, L.; Hovis, J. S.; Boxer, S. G. *Langmuir* **2000**, *16*, 6773–6776.
- (26) Shi, J.; Yang, T.; Cremer, P. S. *Anal. Chem.* **2008**, *80*, 6078–84.

JA904721H